

Highlights

Optimisation of crust freezing in meat processing via Computational Fluid Dynamics

Evaldas Greiciunas, Federico Municchi, Nicodemo Di Pasquale, Matteo Icardi

- Computational model for continuous impingement freezing was developed
- Continuous solid (burger meat) domain undergoes phase-change
- Parametric study shows non-linear freezing behaviour
- The results show a potential of highly optimising the impingement freezing performance

Optimisation of crust freezing in meat processing via Computational Fluid Dynamics

Evaldas Greiciunas^a, Federico Municchi^a, Nicodemo Di Pasquale^b and Matteo Icardi^{a,*}

^a*School of Mathematical Sciences, University of Nottingham, NG7 2RD, UK*

^b*School of Mathematics and Actuarial Science, University of Leicester, LE1 7RH, UK*

ARTICLE INFO

Keywords:

Computational Fluid Dynamics (CFD)
Conjugate Heat Transfer (CHT)
Numerical Analysis
Food Processing
Impingement Freezing

ABSTRACT

In this work a numerical model for two-dimensional axisymmetric continuous freezing by impingement of processed meat or similar products in food industry moving along a conveyor belt is presented. The model represents a more computationally efficient alternative to solve conjugate heat transfer between a fluid and a solid, accompanied by phase change in some constituents of the solid phase. In the model presented here it is assumed that the solid can be represented as an homogeneous medium, with its thermophysical properties depending on the temperature. The impingement freezing model is conceived to be valid for highly processed vegetarians products or meat such as sausages, mince or ham freezing. Furthermore, this approach is much simpler in terms of computational cost whilst it still captures the complexity of continuous freezing under industrial setting. The methodology is implemented as a new solver in the widely used open-source Computational Fluid Dynamics (CFD) library OpenFOAM[®]. Overall, highly non-linear freezing behaviour was found due to the phase change inside the solid and the associated heat of fusion. We studied the effect of high fluid Reynolds numbers as well as investigating the optimal distance between the jet and the solid surface for different speeds of the conveyor. We found that the maximum freezing is obtained positioning the jet at a distance $H = 7.2D$ (where D is the diameter of the impinging jet) and setting the speed of the conveyor such that the Péclet number of the solid is $Pe_s = 8244$. The methodology developed allows to obtain detailed insight on the freezing process for various impingement configurations at a minimum computational cost using a freely available open-source tool.

1. Introduction

An important part of food industry is represented by freezing of produce such as vegetables and meat. Food freezing is a complex problem which needs to take into account several different parameters for a complete description of the process, such as freezing time, food quality, and freezing cost. Historically, commercial freezing of food products was obtained through cryogenic immersion or mechanical freezing [1, 2]. A combination of the two above mentioned processes can also be used: firstly, through cryogenic immersion a rapid formation of a protective layer of the food is accomplished, which functions both as a protection during transportation and prevents losses in the moisture content when subject to slow mechanical freezing [1]. Cryogenic freezing typically uses liquid N_2 or liquid CO_2 [3] and has the highest rate of heat transfer compared to other processes due both to the high temperature gradients between the coolant and the food and because of the evaporation of the refrigerant (latent heat of vaporisation). Additionally, the high rates of heat transfer reached in cryogenic freezing result in the formation (nucleation) of smaller ice crystal inside the solid. This is associated with higher food quality since the ice crystals produced by cryogenic freezing are too small to damage the food structure [4, 5, 6, 7]. However, cryogenic freezing has two main disadvantages: firstly, the sudden freezing induces stresses in the products which can lead to damage [8]. Secondly it is an economically expensive technique because of the volumes of cooling liquid required (up to 1 kg of N_2

per 1 kg of processed product) [9, 3]). Mechanical freezing is cheaper than cryogenic freezing, however, it is less efficient (heat transfer coefficients $h \ll 50 \text{ W}/(\text{m}^2\text{K})$). The reduced heat transfer rate leads to the growth of significantly larger ice crystals and thus to a reduced of quality of the final product [9]. As a result, there is a substantial interest for developing alternative fast low cost food freezing techniques such as Impingement Freezing (IF), High Pressure-assisted Freezing (HPF), Hydrofluidisation Freezing (HF), description of which can be found in [2, 6, 5].

Impingement freezing is essentially an improved mechanical freezer [2] in which cold air jet is perpendicularly directed towards the food. This results in an enhanced heat transfer due to the break-up of the fluid boundary layer next to the solid surface [10]. Traditionally, an impingement freezer for food industry would have the following components (Figure 1a) [9]:

- Freezing chamber.
- Grid or conveyor belt on which the produce is placed and transported.
- One or multiple nozzles which supply high speed cooling air. Nozzles can be installed perpendicularly to the belt or at different angles. Additionally, some nozzles can be placed along the conveyor belt to supply air at different temperatures [11, 6]

It is worth to notice that impingement freezing is one of few new techniques which have been fully commercialised [12, 13, 14] due both to its cost effectiveness compared to cryogenic freezing, and to the significantly lower freezing times

*Corresponding author
ORCID(s):

compared to conventional mechanical freezing. Clearly, air based impingement works best for dense food products with high surface area (since air does provide an efficient heat transfer). However, the process is well suited for rapid surface freezing applications (such as crust freezing) due to its capabilities for fast freezing [2]. It was also shown that for some applications, impingement freezing is able to produce similar freezing time compared to cryogenic freezing (e.g. for small burgers[15]) without the complexity of the cryogenic process. Furthermore, IF is 62-79% faster and with 36-72% reduced weight loss when compared to conventional freezing, thanks to the highest heat transfer coefficients[9]. An experimental study by [3] showed that the heat transfer coefficient ranges between 70 – 250 W/(m²K), depending on the regime of the cooling air. However, it should also be noted that whilst increasing jet velocity reduces the freezing time it could also have damaging effects to the structure of the food [3]. Additional drawbacks of the IF with respect to standard freezing equipment are: the higher installation costs and power consumption. However, these are offset by much faster product processing capabilities [14].

IF is more complex than conventional mechanical freezing both from food product and fluid perspectives, and there is a significant interest in optimising this procedure. The optimisation of this process can be obtained by either experiments or numerical modelling, since analytical relations can only be found for excessively simplified cases. Generally, in experimental works the heat transfer coefficient is measured for both control samples [16] or real food [3] products under impingement conditions. However, such measurements are difficult and experiments tend to be expensive. An interesting scenario was considered by [12], who investigated the optimum jet placement. They found that the best freezing conditions can be obtained by placing the jets at approximately 6-8 jet diameters away from the freezing surface.

Numerical modelling studies usually focus their attention mainly on the food product domain [9, 1, 17, 18, 19]. In these studies, the main objective is the description of the solid freezing process, its various associated parameters such as the mass diffusion, important for porous products (e.g. bread), and its related processes such as recrystallisation [17]. The single solid domain modelling approach requires special boundary conditions, either coolant temperature or a heat transfer coefficient at the boundary corresponding to a certain freezing process. These boundary conditions cannot accurately define complex cooling process of an impinging jet. The computational complexity from modelling both fluid and solid domains resulted in studies which addressed the problem only under certain limiting hypothesis. [20] and [21] examined the effect of impinging jet cooling of a cylindrical food product placed on a conveyor belt (Figure 1a) using Computational Fluid Dynamics (CFD) from a frontal view perspective. In both cases turbulent air was

ρ_f	1.569	kg/m ³
C_p	1002.7	J/(kg K)
μ	1.467×10^{-5}	Pa s
Pr	0.728	-

Table 1

Constant properties of air at $T = 225$ K. Here C_p is the heat capacity and Pr is the (non turbulent) Prandtl number. Notice that the heat conductivity κ is calculated employing the definition $Pr = \rho_f C_p / \kappa$.

modelled using the $k-\omega$ SST model, which is effective in capturing near-wall effects [22] with the results showing highly non-linear heat transfer coefficient along the solid surface. However, in the case of [20] only the solid boundary was modelled whilst [21] used a Conjugate Heat Transfer (CHT) formulation with no phase change. The phase change was omitted purely based on arguments of numerical stability, since the resulting sudden change in thermophysical properties can lead to difficult convergence [17]. This, combined with the non-linear nature of fluid dynamics makes the modelling challenging. An attempt to model both the impinging jet and the solid cooling in axisymmetric coordinates was reported by [23]. However, the lack of numerical details, the computing resolution (12000 cells maximum in total) and overall mesh quality raise some questions regarding the quantitative accuracy of this study.

In this work, a continuous axisymmetric impingement freezing model with CHT is developed for food products. Contrary to current studies, phase change in the solid is modelled using thermophysical properties of burgers obtained from [1]. The model provides a good computational compromise between complexity of fluid dynamics calculations and the phase changing of the solid and is able to predict freezing of continuous dense foods such as sausages, cooked ham, mince. Additionally, the model allows tuning of multiple parameters such as jet diameter, jet distance from food, food velocity whilst taking into account complex freezing and impinging jet processes.

2. Numerical model

2.1. Governing equations for the fluid flow

Numerical modelling was performed in OpenFOAM[®] using a custom solver with its base built on chtMultiregionFoam - a solver for conjugate heat transfer. The fluid flow was modelled using RANS (Reynolds Averaged Navier Stokes) equations closed with a $k-\omega$ SST turbulence model [24]:

$$\nabla \cdot (\rho_f \mathbf{u}) = 0 \quad (1)$$

$$\nabla \cdot (\rho_f \mathbf{u} \mathbf{u}) = -\nabla p_{rgh} + \nabla \cdot \boldsymbol{\tau}_{\text{eff}} - (\mathbf{g} \cdot \mathbf{x}) \nabla \rho_f \quad (2)$$

$$\nabla \cdot (\rho_f \mathbf{u} h_f) = \nabla \cdot (\alpha_{\text{eff}} \nabla h_f) - \rho_f \mathbf{u} \cdot \mathbf{g} + \nabla \cdot (\boldsymbol{\tau}_{\text{eff}} \cdot \mathbf{u}) \quad (3)$$

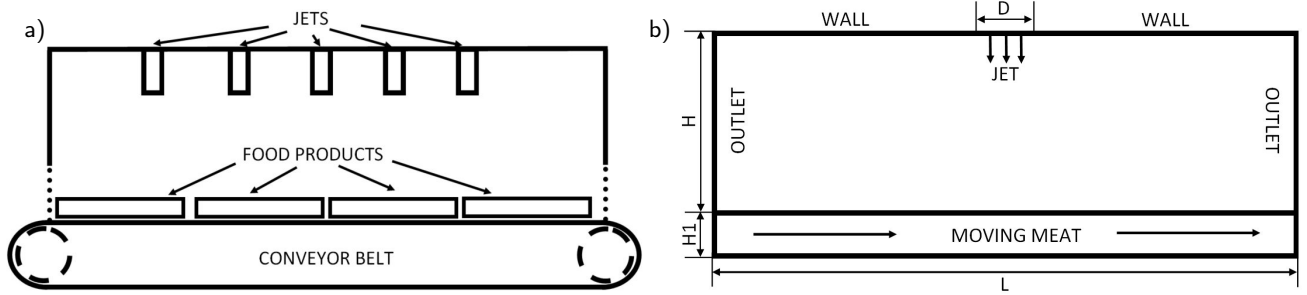


Figure 1: a) Typical impingement freezing setup used in industrial refrigeration [11]. b) Simplified axisymmetric setup for continuous impingement freezing.

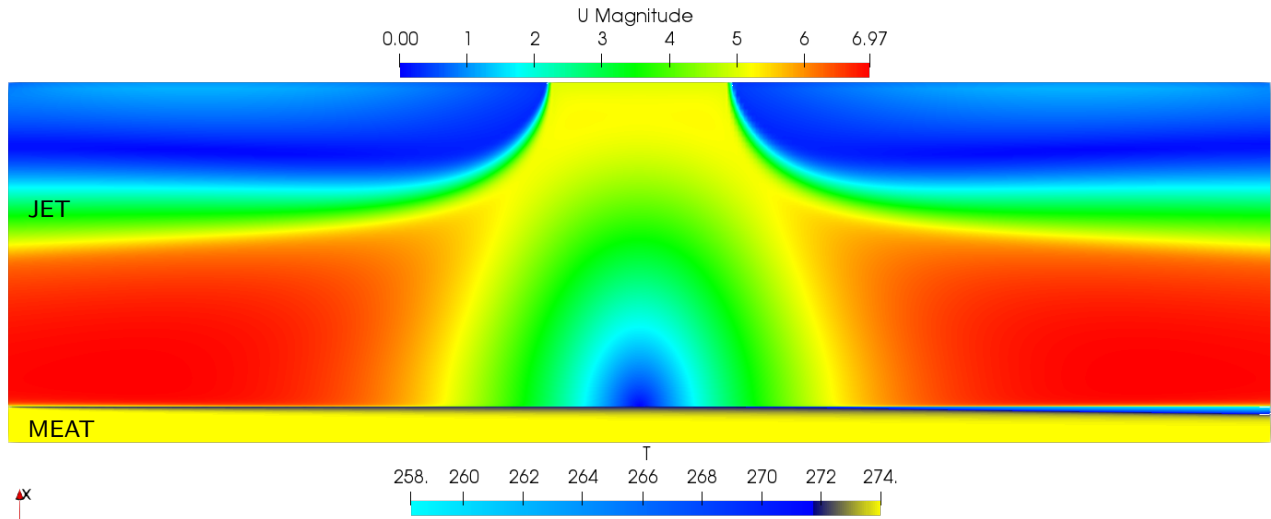


Figure 2: Example jet and solid domain visualisation at Fine2 mesh resolution during mesh independence. For the fluid domain - velocity magnitude contours are used whilst for the solid domain temperature contours are used to highlight the freezing front.

where \mathbf{u} is the fluid velocity field, p_{rgh} is the pressure head, ρ_f is the fluid density, h_f is the fluid enthalpy, \mathbf{g} is the gravitational acceleration, and \mathbf{x} is the spatial coordinate. Furthermore, $\alpha_{\text{eff}} = \alpha_f + \mu_t / (\rho_f \text{Pr}_t)$, where α_f is the effective heat diffusivity of the fluid and Pr_t is the turbulent Prandtl number taken to be 0.85 in RANS simulations. The effective deviatoric stress tensor is given by:

$$\boldsymbol{\tau}_{\text{eff}} = \mu_{\text{eff}} (\boldsymbol{\nabla} \mathbf{u} + \boldsymbol{\nabla}^T \mathbf{u}) \quad (4)$$

With $\mu_{\text{eff}} = \mu + \mu_t$, where μ is the molecular viscosity and μ_t is the dynamic turbulent viscosity and calculated based on the turbulence model [22]. Wall treatment is undertaken using switchable low and high Reynolds wall functions based on the frictional wall distance:

$$y^+ = y \frac{\sqrt{\tau_w \rho_f}}{\mu_{\text{eff}}} \quad (5)$$

Where τ_w is the wall shear stress and y is the distance between the first cell and the wall. The model switches from laminar to turbulent at $y^+ = 11$ [25]. In terms of the fluid properties, incompressible air was used with constant properties at $T = 225$ K (summarised in Table 1). In the study,

Reynolds number of the jet is defined as:

$$\text{Re} = \frac{\rho_f U_{in} D}{\mu} \quad (6)$$

Where U_{in} is the jet inlet velocity and D is the jet diameter (see Figure 1b). This dimensionless number is employed to represent different working conditions of the impingement device.

2.2. Governing equations for the solid

The solid phase is modelled using an enthalpy based energy conservation equation for moving materials.

$$\mathbf{v} \cdot \boldsymbol{\nabla} h_s = \boldsymbol{\nabla} \cdot (\alpha_s \boldsymbol{\nabla} h_s) \quad (7)$$

Here h_s is the solid enthalpy, α_s is the solid heat diffusivity and \mathbf{v} is the conveyor speed in [m/s], \mathbf{v} - a constant one-dimensional velocity along the domain axis, resulting in a computationally efficient model representing motion of solid domain on the conveyor belt. This additional term is implemented as a programmable source term into OpenFOAM®. Furthermore, the formulation presented here allows to obtain a steady-state solution of a rather complex freezing problem

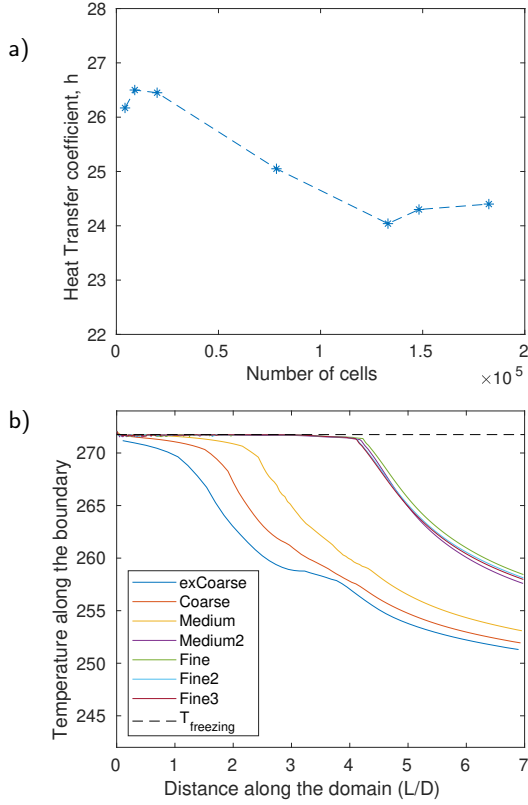


Figure 3: a) Average Heat transfer coefficient h [$W/m^2 K$] at the fluid-solid boundary versus number of cells in different meshes. b) Temperature data along the fluid-solid boundary at various mesh resolutions.

which significantly reduces the computational time. Additionally, a custom thermophysical model was implemented using the thermophysical data for burgers reported in [1], assuming 70% water content throughout the study which results in a freezing temperature of $T_{fz} = 271.7$ K. This thermophysical model in addition to continuous freezing (allowed by the temperature advection term) enables modelling phase change and the associated heat of fusion effects to the freezing front and heat transfer coefficient. Finally, a working parameter for the conveyor is defined: the solid Péclet number:

$$Pe_s = \frac{H1|\mathbf{v}|}{\alpha_s} \quad (8)$$

Where $H1$ is the radial length of the solid (see Figure 1b) and $|\ast|$ indicates the module operator. This dimensionless number allows to parametrise the working conditions of the conveyor.

2.3. Computational Domain and Grid Independence

Computational domain is a simplification of the real process shown in Figure 1a and is illustrated in Figure 1b. It is aimed at studying the non-linear freezing behaviour caused by a jet-solid interaction. The differential operators were dis-

gradient (∇)	Gauss linear
laplacian (∇^2)	Gauss linear corrected
div(phi,U)	Gauss linearUpwindV grad(U)
div(phi,h) (solid)	Gauss linearUpwind grad(h)
div(phi,h) (fluid)	bounded Gauss upwind
div(phi,k)	Gauss upwind
div(phi,omega)	Gauss upwind

Table 2

Discretisation schemes as from the *fvSchemes* OpenFOAM[®] dictionary used for simulations.

Mesh	Number of cells			y^+_{mean}
	Total	Solid	Fluid	
Ex-coarse	4233	663	3570	21.78
Coarse	9000	1500	7500	15.61
Medium	19950	3990	15960	13.38
Medium2	78400	28000	50400	0.72
Fine	133000	49400	83600	0.08
Fine2	148200	49400	98800	0.03
Fine3	182400	49400	133000	0.03

Table 3

Meshes used for the grid independence study.

cretised in the governing equations employing finite volume formulation and the interpolation schemes shown in Table 2. Throughout the study, both jet and solid inlet temperatures were kept constant and equal to $T_{in,f} = 225$ K and $T_{in,s} = 274$ K respectively. The computational domain was built based on the jet diameter D with dimensions respectively equal to: $H1=0.2D$, $H=1.8D$, $L=7D$. Numerical grids were built in OpenFOAM[®] using the *blockmesh* utility, which allows the generation of orthogonal hexahedral meshes. The main variables of the domain kept were the solid and jet velocities as well as the distance of the jet from the solid, allowing to optimise the freezing process for a variety of scenarios explored throughout this work.

2.3.1. Grid Independence

Sensitivity of the solution was investigated with respect to the mesh resolution using the meshes reported in Table 3, with operating conditions defined by: $U_{in} = 5$ m/s and $|\mathbf{v}| = 1$ mm/s. These particular operating conditions result in a large amount of solid material becoming frozen, and they therefore are a good indicator of the robustness of the algorithm. Average heat transfer coefficient h as a function of the grid size was analysed, defined as:

$$h = \frac{\dot{q}_{fs}}{T_{in,f} - T_{fs}} \quad (9)$$

where \dot{q}_{fs} and T_{fs} represents the total heat exchanged and the average temperature at the interface between fluid and solid respectively. It also should be noted that h is the primary measure for evaluating performance. The results reported in Figure 3a show a convergence for the values of h for grids finer than the one indicated as *Fine* in Table 3.

Temperature profile along the fluid-solid interface was

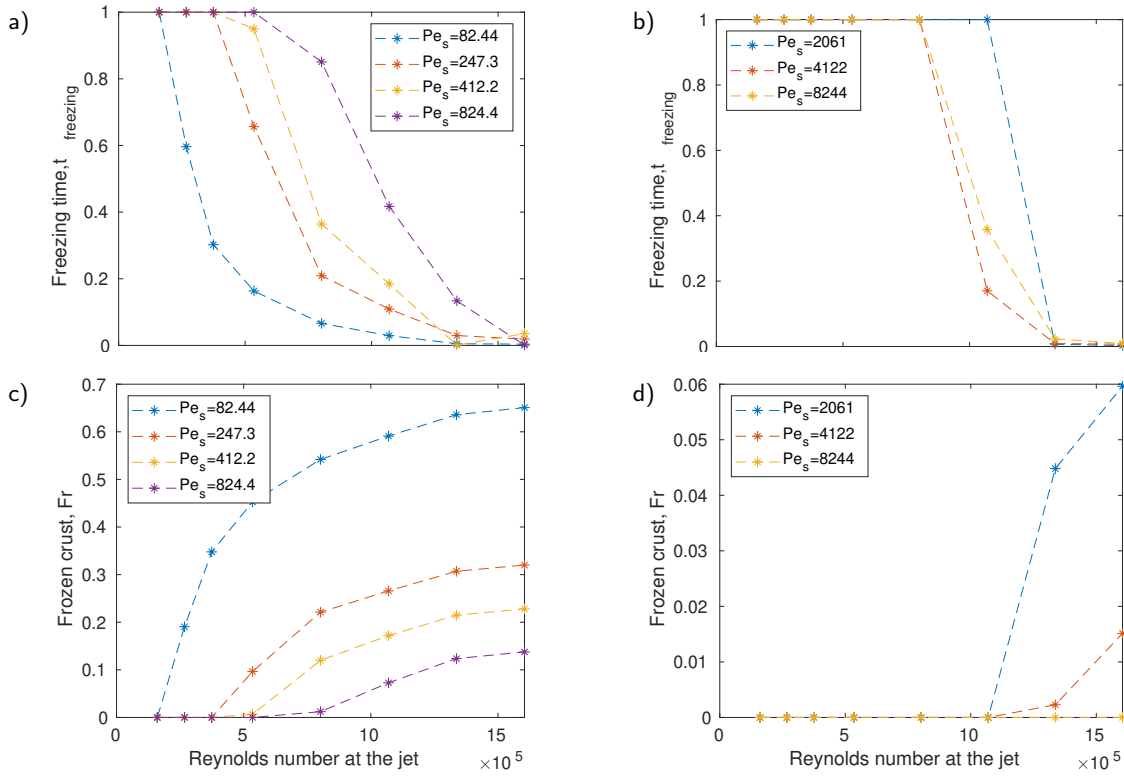


Figure 4: a), b) freezing times associated at various solid Pelet and Reynolds numbers. c), d) Final frozen crust thickness at various solid Pelet and Reynolds numbers. The data is with domain of $H=1.8D$.

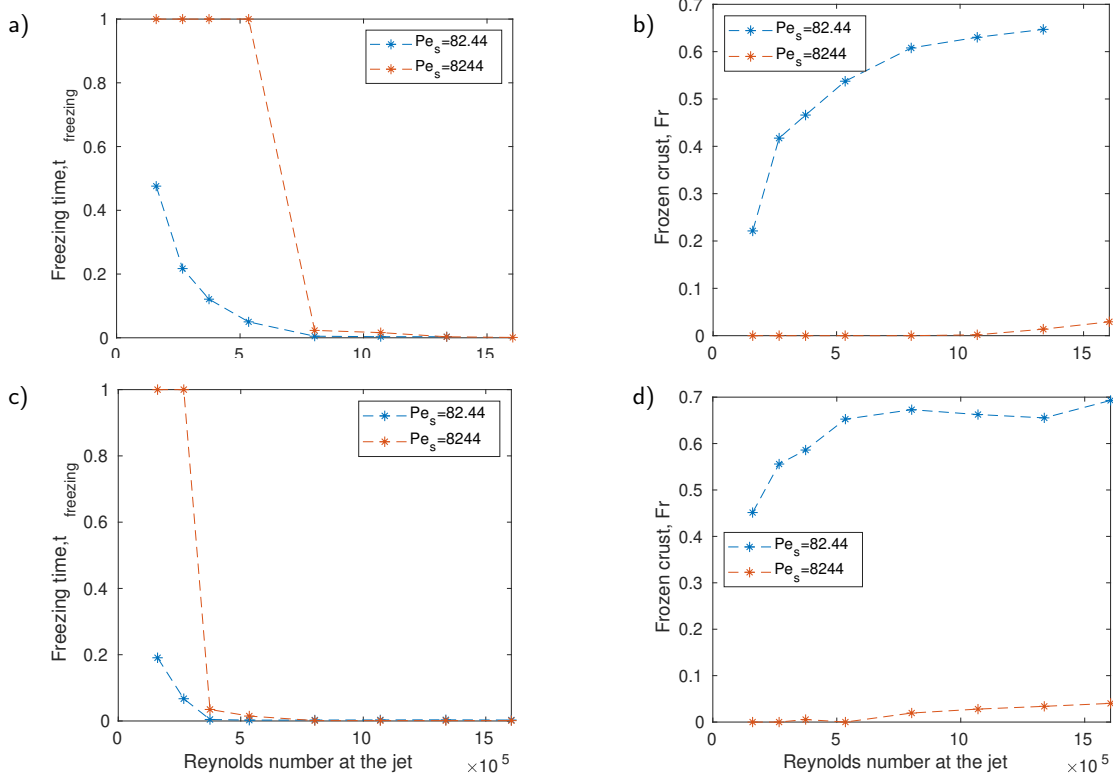


Figure 5: a) Freezing time and b) frozen crust at $H=3.6D$. c) Freezing time and d) frozen crust at $H=7.2D$.

also considered (Figure 3b) which also shows convergence for finer grids.

It can be inferred from Figure 3a, that the three finer grids predict a very similar heat transfer coefficient whilst lower resolution grids tend to overestimate the performance of the heat transfer in the model. This last observation is also clearly represented in Figure 3b, where it is shown that the coarser meshes lead to a rather significant overcooling. As a result it was found that the mesh resolution indicated as *Fine2* (see Table 3) was appropriate to conduct the present study. Figure 2 shows the temperature and velocity fields obtained employing such grid.

3. Results

Parametric study was performed sampling at eight values of Re in the range $1.604 \times 10^5 \leq Re \leq 1.604 \times 10^6$ ($3 \leq U_{in} \leq 30$ m/s) and at seven conveyor speeds in the range $1 \leq |\mathbf{v}| \leq 100$ mm/s. This choice of parameters resulted in a solid Péclet number in the range: $82.44 \leq Pe_s \leq 8244$, allowing to consider a variety of scenarios.

Parameters of interest such as freezing time and the frozen crust thickness were calculated using iso-surfaces of $T = 271$ K in the solid domain (≈ 0.5 K below a freezing point of the solid). The freezing time was calculated by taking the first coordinate of the iso-surface along the axial direction (x_{fz}):

$$t_{fz} = \frac{x_{fz}}{|\mathbf{v}|t_L} = \frac{x_{fz} |\mathbf{v}|}{|\mathbf{v}| L} = \frac{x_{fz}}{L}. \quad (10)$$

Note that, in our definition, the freezing time t_{fz} is a dimensionless quantity obtained by dividing it by the time required for the conveyor to perform one passage through the domain $t = L/|\mathbf{v}|$. It should be noted that the initial stable freezing times at low Reynolds numbers in shown Figures 4a and 4b show that no freezing occurs while the solid is transported through the domain.

The dimensionless frozen crust thickness (y_{fz}) was calculated using the iso-surface radial coordinate at $x = L$ (Figure 1b):

$$Fr = \frac{y_{fz} - H1}{H1} \quad (11)$$

Figures 4c and 4d, show a frozen crust of 0 mm at the lower Reynolds numbers, indicating that the solid did not freeze appreciably, and higher forced convection is required to overcome the latent heat of freezing. However, these results also show that at the highest Reynolds numbers the freezing process is almost instantaneous and leads to a significant frozen crust formation in the majority of the situations. Interestingly, it can be observed that no significant frozen crust is formed at $Pe_s = 8244$, $Pe_s = 4122$ and $Pe_s = 2016$ (Figures 4c and 4d) despite freezing times being sufficiently low, which also show the fact that extra energy is required to overcome the latent heat of freezing.

Heat transfer coefficient for the lowest and highest Péclet numbers considered ($Pe_s = 82.44$ and $Pe_s = 8244$) is

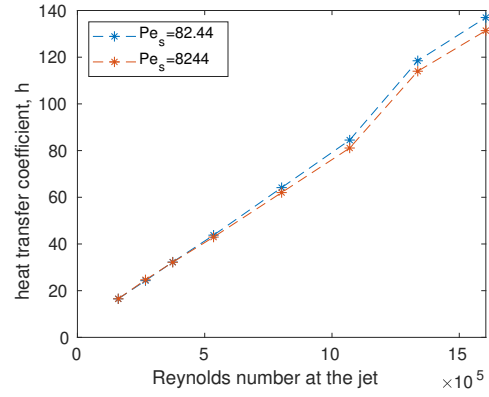


Figure 6: Heat transfer coefficient h [W/m^2K] as function of Reynolds number for two different values of the Péclet number. The data refer to the domain of $H=1.8D$.

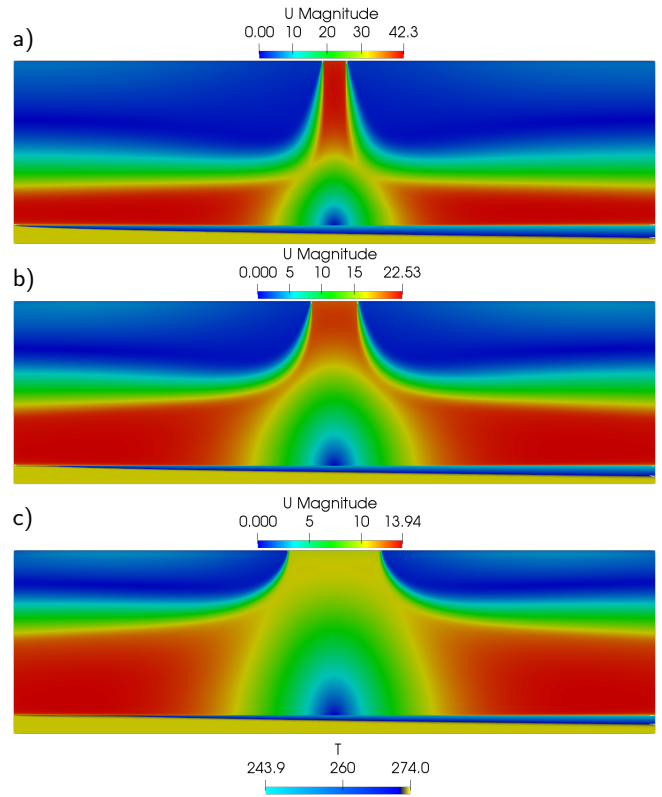


Figure 7: Three computational domains at $Re = 5.348 \times 10^5$, $Pe_s = 82.44$ using jet diameter to distance to the solid ratios of: a) $H/0.25D$ b) $H/0.5D$ c) H/D .

shown in Figure 6. Interestingly, the conveyor speed does not seem to have an appreciable effect on the heat transfer. This result is quite counter intuitive, since one would think that the additional shear created at the fluid-solid interface should increase fluid mixing and consequently increase the heat transfer coefficient. However, it can be explained by the low thermal conductivity of the meat influencing the results. For higher values of the Reynolds number a small decrease in h can be observed together with the increase of the Péclet

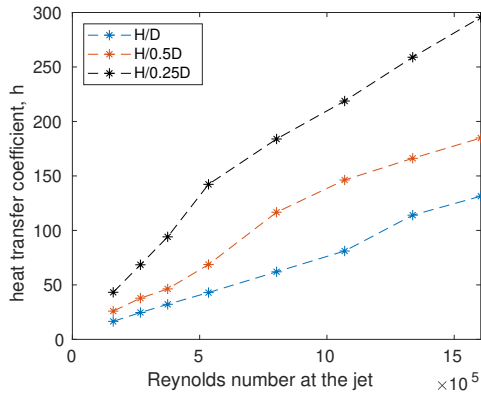


Figure 8: Heat transfer coefficient h [W/m²K] at $Pe_s = 82.44$ using different jet diameter to the distance from the solid.

number. This effect is related to the difference in frozen crust temperature between the two operating conditions. The effect of quick freezing discussed above can also be seen in Figure 6 at the two highest Reynolds numbers, where a change of slope takes place, when the latent heat of fusion at the solid-fluid interface is overcome.

The just discussed results also show that a more detailed analysis is necessary to investigate the two dominant parameters of the impingement freezing domain: jet distance from the solid (H) and solid material thickness (H_1) which are explored using the two limiting values of the Péclet number ($Pe_s = 82.44$ and $Pe_s = 8244$).

3.1. Influence of the jet diameter

The effects of jet distance from the solid have been considered since [12], that reported an optimum jet diameter to distance ratio of 6-8.

In this subsection the computational domain is modified by reducing the jet diameter two and four times ($D_1=0.5D$ and $D_2=0.25D$), effectively obtaining $H=3.6D_1$ and $H=7.2D_2$. It should be noted, that all the other geometrical parameters were left identical to the original domain. This allows to keep a solution similarity.

Simulation results from the three domains are shown in Figure 7 and suggest that, for the same value of the Reynolds number, the further away the jet is from the solid domain the quicker is the freezing process. Additionally, the fluid bulk region develops between the interface and the jet inlet, which is larger for larger values of D . This in turn increases the fluid mixing and heat transfer close to the fluid-solid surface, which results in more efficient freezing. In terms of heat transfer coefficient, this effect is shown in Figure 8. The largest heat transfer coefficient results from moving the jet inlet away from the solid in agreement with results from [12]. In particular, the heat transfer coefficients in the case of $H=7.2D$ is more than doubled than for the $H=1.8D$ domain. Comparing the freezing time and crust thickness (Figure 5), it can be noticed that increasing the distance of the jet from the solid results in both faster freezing time and deeper crust formation. A further increase of the conveyor velocity to the

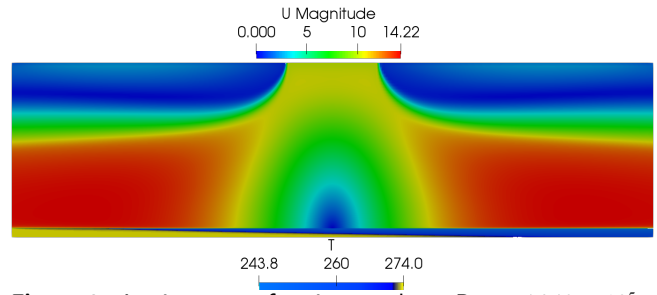


Figure 9: Impingement freezing result at $Re = 5.348 \times 10^5$, $Pe_s = 82.44$ using a 50% thinner solid material domain using a jet diameter to solid distance ratio of $H=3.6D$.

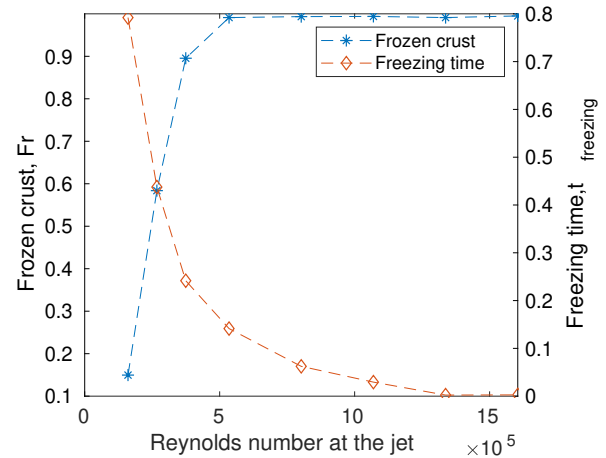


Figure 10: Crust thickness and the freezing time in the half radius domain ($H=0.5H_1$) as a function of the Reynolds number.

maximum Péclet number considered ($Pe_s = 8244$) results in a similar behaviour to the original domain, and thus in the formation of a very thin frozen crust despite an almost instant freezing time. However, for both $H=3.6D$ and $H=7.2D$ the crust is still significantly larger with respect to the case where $H=D$. This last fact opens the possibility to optimise the freezing process by just changing the position of the impinging jet. However, an interesting nonlinear behaviour can be seen at $H=7.2D$ and $Pe_s = 82.44$ (Figure 5d) where a stabilisation in frozen crust thickness is observed at the highest Reynolds numbers. This stabilisation indicates that for a specific solid thickness and conveyor velocity, we can derive a critical *Reynolds jet-to-solid* distance over which the impingement effect sharpens and results in an inefficient cooling.

3.2. Influence of the solid diameter

In this section halving the solid domain diameter (H_1) compared to the previous cases is undertaken to study its influence to the freezing performance. Figure 9 illustrates the results at $Pe_s = 82.44$. Comparison the results in Figure 7c reveals differences between the domains. In the case of a thinner solid, the process is capable of complete freezing

(Figure 9) with a consistent behaviour across a wide range of Reynolds numbers (Figure 10). Compared to the results in Figure 4 at $Pe_s = 82.44$, freezing is observed to take place at lower Reynolds numbers and at shorter axial coordinates. This shows a dependence of the freezing characteristics from the solid diameter and the need for process tuning for different products.

4. Conclusions

A numerical model for axial impingement freezing of food products on a moving conveyor is proposed. The model is able to capture phase change, which is critical in capturing the thermophysical description of the freezing process. The model was implemented in the finite volume open-source library OpenFOAM® as a custom solver and its numerical convergence is presented in an industrial application. Key dimensionless parameters were identified to describe the performance of the freezing model. Additionally, a parametric study to investigate the process efficiency under different operating conditions and geometrical configurations of the potential freezing apparatus was undertaken. The key findings of the study can therefore be summarised by:

- High Reynolds numbers are required to overcome the effects of the latent heat of freezing. The effect becomes more pronounced at high conveyor speeds, in which the large velocity do not leave sufficient time to the frozen layer to penetrate in depth in the solid.
- Freezing time and thickness are dependent on the solid material thickness. By halving the solid domain radius of one half, the complete freezing of the product was found as it moves along the domain. Thus, it requires a significantly lower fluid flow speed and overall heat transfer coefficient.

Future studies may include the investigation of more complicated 3-dimensional geometries as well as the generalisation to heterogeneous and anisotropic food products through the use of improved thermophysical models.

Acknowledgements

The authors would like to thank University of Nottingham Hermes fund for sponsoring the research.

References

- [1] Miriam E. Agnelli and Rodolfo H. Mascheroni. Cryomechanical freezing. A model for the heat transfer process. *Journal of Food Engineering*, 47(4):263–270, 2001.
- [2] Christian James, Graham Purnell, and Stephen J. James. A Review of Novel and Innovative Food Freezing Technologies. *Food and Bio-process Technology*, 8(8):1616–1634, aug 2015.
- [3] V Soto and R B Orquez. Impingement jet freezing of biomaterials. Technical report.
- [4] WEL Spiess. Impact of freezing rates on product quality of deep-frozen foods. *Food Process Engineering, Applied Science, London*, pages 689–694, 1980.
- [5] Tawanda Marazani, Daniel M. Madyira, and Esther T. Akinlabi. Investigation of the Parameters Governing the Performance of Jet Impingement Quick Food Freezing and Cooling Systems – A Review. *Procedia Manufacturing*, 8:754–760, 2017.
- [6] Lilian Daniel Kaale, Trygve Magne Eikevik, Turid Rustad, and Kjell Kolsaker. Superchilling of food: A review, dec 2011.
- [7] KP Poulsen. The freezing process under industrial conditions. *Science et Technique du Froid (IIR)*, 1977.
- [8] G. H. Zhou, X. L. Xu, and Y. Liu. Preservation technologies for fresh meat - A review, sep 2010.
- [9] Viviana O. Salvadori and Rodolfo H. Mascheroni. Analysis of impingement freezers performance. *Journal of Food Engineering*, 54(2):133–140, sep 2002.
- [10] M Newman. Cryogenic impingement freezing utilizing atomized liquid nitrogen for the rapid freezing of food products. In *Rapid Cooling of food, Meeting of IIR Commission C*, volume 2, pages 145–151, 2001.
- [11] Ron C Lee and Michael K Sahm. Impingement jet freezer and method, April 21 1998. US Patent 5,740,678.
- [12] A Sarkar and RP Singh. Modeling flow and heat transfer during freezing of foods in forced airstreams. *Journal of food science*, 69(9):E488–E496, 2004.
- [13] Arnab Sarkar and R. Paul Singh. Air impingement technology for food processing: Visualization studies. *LWT - Food Science and Technology*, 37(8):873–879, 2004.
- [14] N Winney. From the field to the supermarket—post harvest cooling, part 2 of 4. *Cold Chain*, 2012:20–26, 2012.
- [15] S Sundsten, A Andersson, and E Tornberg. The effect of the freezing rate on the quality of hamburgers. In *Rapid cooling of food, meeting of IIR Commission C*, volume 2, page 2001, 2001.
- [16] Brent A Anderson and R Paul Singh. Effective heat transfer coefficient measurement during air impingement thawing using an inverse method. *International Journal of Refrigeration*, 29(2):281–293, 2006.
- [17] Q. Tuan Pham. Modelling heat and mass transfer in frozen foods: a review, sep 2006.
- [18] Ferruh Erdogdu, Arnab Sarkar, and R Paul Singh. Mathematical modeling of air-impingement cooling of finite slab shaped objects and effect of spatial variation of heat transfer coefficient. *Journal of Food Engineering*, 71(3):287–294, 2005.
- [19] Q Tuan Pham. Freezing time formulas for foods with low moisture content, low freezing point and for cryogenic freezing. *Journal of Food Engineering*, 127:85–92, 2014.
- [20] EEM Olsson, LM Ahrne, and AC Trägårdh. Heat transfer from a slot air jet impinging on a circular cylinder. *Journal of Food Engineering*, 63(4):393–401, 2004.
- [21] Carmela Dirita, Maria Valeria De Bonis, and Gianpaolo Ruocco. Analysis of food cooling by jet impingement, including inherent conduction. *Journal of Food Engineering*, 81(1):12–20, jul 2007.
- [22] Florian R Menter, Martin Kuntz, and Robin Langtry. Ten years of industrial experience with the sst turbulence model. *Turbulence, heat and mass transfer*, 4(1):625–632, 2003.
- [23] M Jafari and P Alavi. Analysis of food freezing by slot jet impingement. *Journal of Applied Sciences*, 8(7):1188–1196, 2008.
- [24] Subrahmanyam Chandrasekhar. *Hydrodynamic and hydromagnetic stability*. Courier Corporation, 2013.
- [25] Frank M. White. *Fluid Mechanics*. Mcgraw-Hill, 2011.